

Activation of Ligand Reactivity: Thiolate C–S and Dithiophosphate Ester C–O Heterolyses within a Dimolybdenum(V) System

Edith I. Koffi-Sokpa, D. Troy Calfee, Brian R. T. Allred, Jackie L. Davis, Elaine K. Haub, Alexis K. Rich, Richard A. Porter, Mark S. Mashuta, John F. Richardson, and Mark E. Noble*

Department of Chemistry, University of Louisville, Louisville, Kentucky 40292

Received November 11, 1998

Ligand reactivity was demonstrated for sulfide alkylation, thiolate dealkylation, and dithiophosphate de-esterification within molybdenum(V) dimers. The cationic complex $[\text{Mo}_2(\text{NC}_6\text{H}_4\text{Me})_2(\text{S}_2\text{P}(\text{OEt})_2)_2(\mu\text{-O}_2\text{CMe})(\mu\text{-SR})_2]^+$ was inductively activated toward thiolate C–S and dithiophosphate C–O heterolyses. The dealkylations were studied using anionic nucleophiles, and various reactivity patterns were characterized. The de-esterification of the diethyl dithiophosphate ligands produced complexes containing the rare monoester $\text{EtO}(\text{O})\text{PS}_2^{2-}$ ligand. This ligand's phosphoryl group was poorly nucleophilic but weakly basic. Crystallographic comparisons between the activated cation and the neutral complex $[\text{Mo}_2(\text{NC}_6\text{H}_4\text{Me})_2(\text{S}_2\text{P}(\text{OEt})_2)_2(\mu\text{-O}_2\text{CMe})(\mu\text{-S})(\mu\text{-SMe})]$ were conducted to delineate structural differences related to the activation. A crystallographic study was also done of the complex $[\text{Mo}_2(\text{NC}_6\text{H}_4\text{-CH}_3)_2(\text{S}_2\text{P}(\text{OEt})_2)(\text{S}_2\text{P}(\text{O})\text{OEt})(\mu\text{-O}_2\text{CMe})(\mu\text{-SEt})_2]$, which provided internal comparison of monoester $\text{EtO}(\text{O})\text{PS}_2^{2-}$ and diester $(\text{EtO})_2\text{PS}_2^{2-}$ ligand types.

Introduction

The reactivity of ligands within metal complexes is an area of fundamental importance to many areas of chemistry. The notion of ligand reactivity refers to changes in the chemical identity of a ligand and not merely to ligand migration or dissociation, although these processes can occur with the chemical transformation. Virtually by definition, most metal-catalyzed processes are ligand reactions.

Among the various kinds of ligand reactions, bond scissions are a critically important type. These reactions are the primary function for many transition metal catalysts including enzymes. The catalytic effect is obtained from electronic and/or steric activation of the relevant bonds as a result of coordination of the ligand to the metal center. Studies of the manner by which this activation is accomplished will help to understand these important processes.

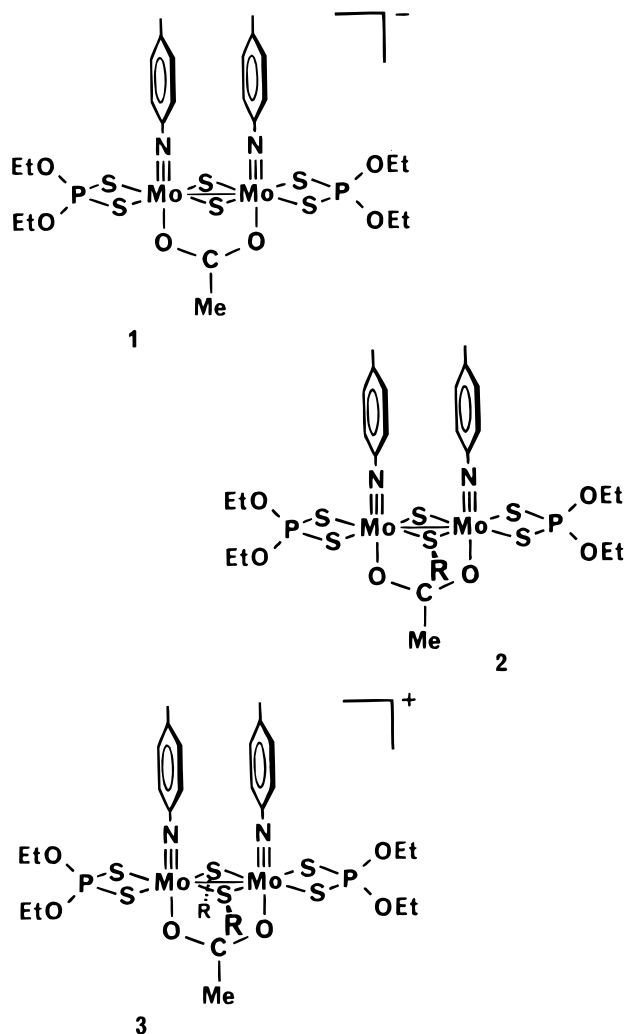
The present work involves heterolytic C–S and C–O cleavage within thiolate ligands and dithiophosphate ester ligands, respectively. These types of ligand reactions are of considerable impact for a broad spectrum of inorganic and organic areas encompassing such diverse topics as hydrodesulfurization, biochemistry, tribology, environmental chemistry, and agricultural chemistry. The hydrodesulfurization interest stems from its massive importance in fossil fuel processing and the need therein to catalytically cleave C–S bonds of organosulfur components.^{1–3} Phosphate ester cleavage is an area of tremendous interest in general, and P–O and C–O scissions are possible depending on the system. Biological aspects of phosphoester cleavage are especially important, although these derivatives are primarily esters of orthophosphate and its

condensed oligomers. Nevertheless, thiophosphate and dithiophosphate compounds are very widespread in their many applications. The interest in the thio derivatives has also extended to biological PO_4^{3-} esters, since sulfur analogues of the natural phosphoesters have been under study in biochemical and biomedical arenas.^{4–6} In tribology, metal complexes of dithiophosphate diesters have been employed for many years as lubrication components in many applications including automobile engines;^{7–10} the breakdown of these compounds during service is an aspect of critical concern. Organic thio/dithiophosphate compounds are also of widespread importance agriculturally and environmentally due to their massive use as pesticides.^{11,12} Their degradation modes are of obvious significance to their pesticidal qualities and to their residual fate, and the environmental ubiquity of metal elements stands to contribute in some way.¹³

- (1) Whitehurst, D. D.; Isoda, T.; Mochida, I. *Adv. Catal.* **1998**, *42*, 345–471.
- (2) Startsev, A. N. *Catal. Rev.—Sci. Eng.* **1995**, *37*, 353–423.
- (3) Chianelli, R. R.; Daage, M.; Ledoux, M. J. *Adv. Catal.* **1994**, *40*, 177–232.

- (4) Okruszek, A.; Olesiak, M.; Krajewska, D.; Stec, W. J. *J. Org. Chem.* **1997**, *62*, 2269–2272.
- (5) Seeberger, P. H.; Yau, E.; Caruthers, M. H. *J. Am. Chem. Soc.* **1995**, *117*, 1472–1478. Seeberger, P. H.; Jorgensen, P. N.; Bankaitis-Davis, D. M.; Beaton, G.; Caruthers, M. H. *J. Am. Chem. Soc.* **1996**, *118*, 9562–9566.
- (6) Martin, S. F.; Wagman, A. S. *J. Org. Chem.* **1993**, *58*, 5897–5899.
- (7) Jiang, S.; Frazier, R.; Yamaguchi, E. S.; Blanco, M.; Dasgupta, S.; Zhou, Y.; Cagin, T.; Tang, Y.; Goddard, W. A., III. *J. Phys. Chem. B* **1997**, *101*, 7702–7709. Jiang, S.; Dasgupta, S.; Blanco, M.; Frazier, R.; Yamaguchi, E. S.; Tang, Y.; Goddard, W. A., III. *J. Phys. Chem.* **1996**, *100*, 15760–15769.
- (8) Willermet, P. A.; Dailey, D. P.; Carter, R. O., III; Schmitz, P. J.; Zhu, W. *Tribol. Int.* **1995**, *28*, 177–187.
- (9) Mortier, R. M.; Orszulik, S. T., Eds. *Chemistry and Technology of Lubricants*; Blackie and Son: Glasgow (VCH Publishers: New York), 1992.
- (10) Colclough, T. *Ind. Eng. Chem. Res.* **1987**, *26*, 1888–1895.
- (11) Eto, M. *Organophosphorus Pesticides: Organic and Biological Chemistry*; CRC Press: Cleveland, 1974.
- (12) Toy, A. D. F.; Walsh, E. N. *Phosphorus Chemistry in Everyday Living*; American Chemical Society: Washington, DC, 1987.
- (13) Hong, F.; Pehkonen, S. *J. Agric. Food Chem.* **1998**, *46*, 1192–1199.

The specific system of study in the present work is a series of dimolybdenum(V) complexes. The starting point in the series is the anionic imido-dithiophosphate-carboxylate-sulfido-molybdenum(V) dimer $[\text{Mo}_2(\text{NAr})_2(\text{S}_2\text{P}(\text{OEt})_2)_2(\mu\text{-O}_2\text{CMe})(\mu\text{-S})]^-$, **1** (Ar = *p*-tolyl). As reported,^{14,15} this complex is potentially nucleophilic toward a variety of substrates; alkyl halides give facile *S*-alkylation at one bridge site to produce neutral μ -thiolate- μ -sulfide complexes $[\text{Mo}_2(\text{NAr})_2(\text{S}_2\text{P}(\text{OEt})_2)_2(\mu\text{-O}_2\text{CMe})(\mu\text{-SR})(\mu\text{-S})]$, **2**. Subsequent studies showed that the remaining



sulfide bridge site in **2** was incompletely passivated and there remained some electron density for further reaction. This was made evident by the sulfide's ability to act as a charge transfer donor to elemental halogen¹⁶ and by the sulfide's vulnerability to oxygenation to give μ -SO and photosensitive μ -SO₂ dimers.¹⁷ These results prompted an investigation into the nucleophilicity of the bridge sulfide in **2** toward alkyl halides, leading to the present work. The expected bis- μ -thiolate cationic complexes $[\text{Mo}_2(\text{NAr})_2(\text{S}_2\text{P}(\text{OEt})_2)_2(\mu\text{-O}_2\text{CMe})(\mu\text{-SR})_2]^+$, **3**, were indeed obtained but with a very curious complication: these products demonstrated an activation toward heterolyses of a bridge thiolate C-S bond and a dithiophosphoester C-O bond. This

paper combines studies of both chemical reactivity and crystallographic structures to investigate the nature of these ligand activations.

In addition to the potential contribution to general aspects of ligand reactivity and to the applications cited above, the dithiophosphate dealkylation produced complexes with the monoethyl dithiophosphate ligand, $\text{EtO}(\text{O})\text{PS}_2^-$. This provided an additional interest from a more basic viewpoint: although a plethora of metal complexes with monoanionic, diester dithiophosphate ligands, $(\text{RO})_2\text{PS}_2^-$, have been known for many years,¹⁸⁻²⁰ complexes with dianionic, monoester ligands, $\text{RO}(\text{O})\text{PS}_2^-$, are very few in number.^{18,21} In fact, the monoester dithiophosphate functionality remains a relative rarity in general. Despite the extensive development of a multitude of diester dithiophosphoric acids, $(\text{RO})_2\text{PS}_2\text{H}$, which ultimately trace to the 1800s,^{22,23} the monoester diacids ROPOS_2H_2 are elusive ("nonexistent"²³) although these have been proposed in some reactions.²⁴ Simple salts have been reported recently for nucleoside monoesters; these are stable at low temperature (dry) but subject to hydrolysis (pH-dependent) in solution.^{4,5} The stabilization of the monoester dithiophosphate group as a ligand provides an opportunity for study, again combining chemical reactivity and structural aspects.

Experimental Section

Reactions and manipulations were conducted open to air except as noted. $[\text{Mo}_2(\text{NTO})_2(\text{S}_2\text{P}(\text{OEt})_2)_2(\text{O}_2\text{CMe})\text{S}(\text{SR})]$, **2**, R = Et²⁵ and Bz,¹⁵ were prepared as previously reported; for **2**, R = Me, the synthesis followed the prior method¹⁷ but used MeI instead of MeBr. Where indicated, dry CH_2Cl_2 and acetone were simply syringed from settled slurries of solvent and drying agent (CaCl_2 and MgSO_4 , respectively). $\text{Bu}_4\text{P}^+ \text{Cl}^-$ was used as a solution (0.45 M) in dry acetone prepared in a glovebag under N_2 . $\text{PPN}^+ \text{Br}^-$ and $\text{PPN}^+ \text{I}^-$ were synthesized by reported methods.²⁶ Other solvents and reagents were used as received. $^{31}\text{P}\{^1\text{H}\}$ and ^1H NMR spectra were obtained on a Varian XL-300 spectrometer (later modified with an Inova300 console) at 121 and 300 MHz, or a Bruker AMX-500 spectrometer at 202 and 500 MHz; results are reported as downfield shifts from external 85% H_3PO_4 and internal Me_4Si . The solvent was CDCl_3 unless otherwise specified. In the NMR characterization data listed below, values for minor sulfur invertomers are given in parentheses in the cases where these could be separately distinguished. Infrared data were obtained using a Mattson Galaxy Series FTIR 5000 spectrometer by diffuse reflectance on KBr powder mixtures. Galbraith Laboratories, Inc. (Knoxville, TN), performed the elemental analyses.

$[\text{Mo}_2(\text{NTO})_2(\text{S}_2\text{P}(\text{OEt})_2)_2(\text{O}_2\text{CMe})(\text{SM}_2\text{E})_2]^+ \text{CF}_3\text{SO}_3^-$, **3** (R = Me) CF_3SO_3^- . In a glovebag under N_2 , $\text{CF}_3\text{SO}_3\text{Me}$ (12.5 μL , 0.11 mmol) was added to an orange slurry of $[\text{Mo}_2(\text{NTO})_2-$

(14) Lizano, A. C.; Noble, M. E. *Inorg. Chem.* **1988**, *27*, 747-749.

(15) Noble, M. E. *Inorg. Chem.* **1986**, *25*, 3311-3317.

(16) Lee, J. Q.; Sampson, M. L.; Richardson, J. F.; Noble, M. E. *Inorg. Chem.* **1995**, *34*, 5055-5064.

(17) Wang, R.; Mashuta, M. S.; Richardson, J. F.; Noble, M. E. *Inorg. Chem.* **1996**, *35*, 3022-3030.

(18) Haiduc, I.; Sowerby, D. B.; Lu, S.-F. *Polyhedron* **1995**, *14*, 3389-3472.

(19) Mehrotra, R. C.; Srivastava, G.; Chauhan, B. P. S. *Coord. Chem. Rev.* **1984**, *55*, 207-259.

(20) Wasson, J. R.; Woltermann, G. M.; Stoklosa, H. J. *Fortschr. Chem. Forsch.* **1973**, *35*, 65-129.

(21) Haiduc, I.; Sowerby, D. B. *Polyhedron* **1995**, *15*, 2469-2521.

(22) Chadwick, D. H.; Watt, R. S. In *Phosphorus and its Compounds*; van Wazer, J. R., Ed.; Interscience Publishers: New York, 1961; Vol. 2, pp 1221-1279.

(23) Ailman, D. E.; Magee, R. J. *Organic Phosphorus Compounds*; John Wiley and Sons: New York, 1976; Vol. 7, pp 487-805.

(24) Fridland, S. V.; Shaikhiev, I. G.; Mukhutdinov, A. A.; Il'yasov, A. V.; Musin, R. Z. *J. Gen. Chem. USSR* **1991**, *61*, 575-578.

(25) Noble, M. E. *Inorg. Chem.* **1987**, *26*, 877-882.

(26) Martinsen, A.; Songstad, J. *Acta Chem. Scand. A* **1977**, *31*, 645-650.

(S₂P(OEt)₂)₂(O₂CMe)S(SMe)], **2** (R = Me; 0.0913 g, 0.100 mmol) in 1.0 mL of dry Et₂O. The stoppered flask was removed from the glovebag, and the mixture was stirred for 10 min to give a yellow slurry. This was opened to air, and 2 mL of Et₂O was added. The slurry was filtered, and the solid was rinsed (Et₂O) and dried to give a yellow powder (0.0981 g, 91%). ³¹P NMR (ppm): (110.5), 109.4. ¹H NMR (ppm): (6.78 d), (6.70 d), 6.66 d, 6.46 d, To-H; 4.2–4.0 m, POCH₂; (3.52 s), 2.67 s, (2.54 s), SCH₃; (2.18 s), 2.16 s, To-CH₃; 1.54 s, O₂CCH₃; 1.39 t, 1.23 t, (1.21 t), POCCH₃. Invertomer ratio: 3:1.

[Mo₂(NTO)₂(S₂P(OEt)₂)₂(O₂CMe)(SEt)₂]⁺ CF₃SO₃⁻, **3** (R = Et) CF₃SO₃⁻. In a glovebag under N₂, CF₃SO₃Et (73 μL, 0.56 mmol) was added to a slurry of [Mo₂(NTO)₂(S₂P(OEt)₂)₂(O₂CMe)S(SEt)], **2** (R = Et; 0.4628 g, 0.500 mmol) in 0.6 mL of dry CH₂Cl₂ and 2.5 mL of dry Et₂O. The stoppered flask was removed from the glovebag, and the mixture was stirred for 2.5 h. This was opened to air, and 2.5 mL of Et₂O was added. The slurry was filtered; the product was rinsed (Et₂O) and dried to give a yellow powder (0.5108 g, 93%). Anal. Calcd for Mo₂C₂₉H₄₇F₃N₂O₉P₂S₇: C, 31.6; H, 4.3; N, 2.5. Found: C, 31.0; H, 4.3; N, 2.1. ³¹P NMR (ppm): 110.2, (109.6). ¹H NMR (ppm): 6.75 d, 6.71 d, (6.68 d), (6.61 d), To-H; 4.2–4.0 m, POCH₂; 3.74 q, (2.79 q), 2.64 q, SCH₂; (2.19 s), 2.16 s, To-CH₃; 2.04 t, (1.91 t), 1.90 t, SCCH₃; (1.52 s), 1.41 s, O₂CCH₃; 1.40 t, 1.38 t, 1.25 t, 1.22 t, POCCH₃. Invertomer ratio: 0.95.

[Mo₂(NTO)₂(S₂P(OEt)₂)(S₂P(O)OEt)(O₂CMe)(SEt)₂], **4** (R = Et). A solution of [Mo₂(NTO)₂(S₂P(OEt)₂)₂(O₂CMe)S(SEt)], **2** (R = Et; 0.200 g, 0.216 mmol), and EtI (0.19 mL, 2.4 mmol) in CHCl₃ (3.5 mL) was stirred at 50 °C for 4 h. The solution was then rotavapped. The golden residue was extracted thrice with a solution of Et₂O/hexanes (2:1, 22 mL). The residue was then dissolved in a small volume of *tert*-amyl alcohol and chromatographed on alumina using *tert*-amyl alcohol as eluent. The middle of the first band was collected and rotavapped. The oily residue was extracted with Et₂O/hexanes (2:1, 5 mL) to give a solid, which was filtered off, washed (hexanes), and dried. The isolated product was a yellow solid (0.0481 g, 24%) containing **4** (R = Et) as a single phosphoryl isomer and as a 1:1 solvate with *tert*-amyl alcohol. Anal. Calcd for Mo₂C₂₆H₄₂N₂O₆P₂S₆·C₅H₁₁OH: C, 36.8; H, 5.4; N, 2.8. Found: C, 36.7; H, 5.5; N, 3.0. ³¹P NMR (ppm): (112.5), 112.3, (EtO)₂P; (77.2), 76.7, EtO(O)P. ¹H NMR (ppm): 6.65 d, 6.58 d, 6.53 d, 6.46 d, To-H; 4.15 dq, 4.03 dq, P(OCH₂)₂; 3.84 dq, PO(OCH₂)₂; (3.64 dq), (3.51 dq), 2.89 dq, (2.75 dq), 2.65 dq, (2.56 dq), SCH₂; (2.17 s), 2.13 s, 2.07 s, To-CH₃; (1.96 t), 1.85 t, SCCH₃; 1.51 q, 1.20 s, 0.92 t, *tert*-amyl alcohol; 1.42 s, O₂CCH₃; 1.35 t, 1.21 t, P(OCCH₃)₂; 1.05 t, PO(OCCH₃). Invertomer ratio: 3.

[Mo₂(NTO)₂(S₂P(OEt)₂)(S₂P(O)OEt)(O₂CMe)(SBz)₂], **4** (R = Bz). A solution of [Mo₂(NTO)₂(S₂P(OEt)₂)₂(O₂CMe)S(SBz)], **2** (R = Bz; 0.200 g, 0.203 mmol), and BzBr (0.12 mL, 1.0 mmol) in CHCl₃ (3.0 mL) was stirred at 50 °C for 4.5 h. The procedure hereafter followed that for R = Et above. The product was a yellow solid (0.0723 g, 34%). ³¹P NMR (ppm): (111.6), 111.5, (EtO)₂P; 77.1, EtO(O)P. The ¹H NMR spectrum showed several minor components which were indistinguishable as sulfur invertomers of the dominant phosphoryl isomer or as a minor phosphoryl isomer; only the dominant phosphoryl isomer data are given. ¹H NMR (ppm): 7.75 d, 7.52 t, 7.41 m, Bz-H; 6.55 d, 6.47 d, 6.44 d, 6.36 d, To-H; 4.26 dq, 4.08 dq, P(OCH₂)₂; 4.13 d, 3.76 d, Bz-CH₂; 3.86 dq, PO(OCH₂)₂; (2.10 s), 2.07 s, 2.02 s, To-CH₃; 1.54 s, O₂CCH₃; 1.42 t, 1.24 t, P(OCCH₃)₂; 1.07 t, PO(OCCH₃). Invertomer ratio: ~15.

Bu₄P⁺ [Mo₂(NTO)₂(S₂P(O)OEt)₂(O₂CMe)(SEt)₂]⁻ Bu₄P⁺, **5** (R = Et). A solution of [Mo₂(NTO)₂(S₂P(OEt)₂)₂(O₂CMe)

Table 1. Crystallographic Data

	2	3 CF ₃ SO ₃ ⁻	4
formula	Mo ₂ C ₂₅ H ₄₀ - N ₂ O ₆ P ₂ S ₆	Mo ₂ C ₂₇ H ₄₃ - N ₂ O ₉ P ₂ S ₇ F ₃	Mo ₂ C ₂₆ H ₄₂ N ₂ O ₆ - P ₂ S ₆ ·0.83CDCl ₃
fw	910.8	1074.9	1024.8
cryst syst	triclinic	orthorhombic	monoclinic
space group	<i>P</i> $\bar{1}$ (No. 2)	<i>Pbca</i> (No. 61)	<i>P2₁/c</i> (No. 14)
<i>a</i> , Å	11.006(2)	26.051(7)	14.925(3)
<i>b</i> , Å	14.159(4)	21.049(8)	15.487(3)
<i>c</i> , Å	14.547(4)	16.107(5)	20.404(4)
α , deg	105.83(2)		
β , deg	105.69(2)		108.73(2)
γ , deg	107.76(2)		
<i>V</i> , Å ³	1916(1)	8832(4)	4466(1)
<i>Z</i>	2	8	4
μ , cm ⁻¹	11.01	10.28	11.29
<i>T</i> , °C	23(1)	23(1)	23(1)
λ , Å	0.710 69	0.710 69	0.710 69
ρ (calcd), g/cm ³	1.579	1.617	1.524
<i>R</i> ^a	0.038	0.051	0.047
<i>R</i> _w ^b	0.043	0.052	0.058

$$^a R = \sum ||F_o| - |F_c|| / \sum |F_o|, \quad ^b R_w = [\sum w(|F_o| - |F_c|)^2 / \sum w|F_o|^2]^{1/2}.$$

(SEt)₂]⁺ CF₃SO₃⁻, **3** (R = Et; 0.2205 g, 0.200 mmol), in dry acetone (0.10 mL) was treated with Bu₄P⁺ Cl⁻/acetone (1.3 mL, 0.45 M, 0.58 mmol) in a glovebag under N₂. The stoppered flask was removed from the glovebag, and the solution was stirred for 32 h. Then exposed to air, the resulting yellow-orange slurry was filtered and the solid was washed (acetone/petroleum ether, 2:1 then 1:1) and dried to give a yellow product (0.0706 g, 31%) of a single phosphoryl isomer. Anal. Calcd for Mo₂C₄₀H₇₃N₂O₆P₃S₆: C, 41.6; H, 6.4; N, 2.4. Found: C, 41.0; H, 6.6; N, 2.3. ³¹P NMR (ppm): (80.2), 80.0, EtO(O)P; 33.5, Bu₄P⁺. ¹H NMR (ppm): 6.55 d, (6.46 d), 6.41 d, To-H; 3.70 dq, POCH₂; (3.58 q), 2.71 q, (2.60 q), SCH₂; 2.33 m, PCH₂; (2.08 s), 2.04 s, To-CH₃; (1.96 t), 1.81 t, SCCH₃; 1.52 m, PCCH₂ + PCCCH₂; 1.37 s, (1.29 s), O₂CCH₃; 0.96 t, PCCCCH₃; 0.91 t, POCCH₃. Invertomer ratio: 2.7.

Reactions of RS{Mo₂}S with RX. A typical reaction employed 25 μmol of RS{Mo₂}S **2** and 500 μmol of RX in 1.0 mL of CDCl₃. Reactions were monitored by NMR spectroscopy.

Reactions of EtS{Mo₂}SEt⁺ or RS{Mo₂}S with Nucleophiles. A typical reaction employed 16 μmol of EtS{Mo₂}SEt⁺ CF₃SO₃⁻ (**3** CF₃SO₃⁻) or 16 μmol of EtS{Mo₂}S **2** with 48 μmol of PPN⁺ X⁻ in 1.6 mL of *d*₆-acetone. For the reaction using (EtO)₂PS₂⁻, excess salt was prepared in situ using 60 μmol of (EtO)₂PS₂H + 60 μmol of Et₃N in *d*₆-acetone, diluting to 2.0 mL. Then 16 μmol of EtS{Mo₂}SEt⁺ CF₃SO₃⁻ was dissolved in 1.6 mL of this solution. All reactions were monitored by NMR spectroscopy.

Reactions of EtS{Mo₂(PO)₂}SEt⁻ with Electrophiles. The reaction of Bu₄P⁺ EtS{Mo₂(PO)₂}SEt⁻ (Bu₄P⁺ **5**; 16 μmol) with CF₃SO₃Me (16 μmol) was conducted in CDCl₃ (1.0 mL). The incremental reaction of Bu₄P⁺ EtS{Mo₂(PO)₂}SEt⁻ (17.3 μmol) with HBF₄·Et₂O (85%) was conducted in CDCl₃ (0.86 mL), followed by neutralization using 2,6-lutidine. All reactions were monitored by NMR spectroscopy.

Crystallography. Crystal data and experimental details are shown in Table 1. Data were collected on an Enraf-Nonius CAD4 automated diffractometer with Mo K α radiation (graphite monochromator), using the ω - 2θ scan technique. Computations utilized the teXsan software packages.²⁷ Absorption corrections and Lorentz and polarization corrections were applied in each case. Scattering and anomalous dispersion factors were taken

(27) *teXsan: Crystal Structure Analysis Package*; Molecular Structure Corp.: the Woodlands, TX, 1985, 1992.

from ref 28. Structures were solved by Patterson methods and expanded using Fourier techniques. Hydrogen atoms were calculated and included as fixed contributions, but these were not further refined. Each structure was refined by full-matrix, least-squares methods minimizing $\sum w(|F_o| - |F_c|)^2$, where $w = [\sigma^2(F)]^{-1}$. Each structure contained some disorder within the dithiophosphate ethoxy groups, which has been common within related dimolybdenum complexes.^{16,17,29} Although this was unfortunate in this work due to the interest in the dithiophosphate ligands themselves, the disorders limited but did not eliminate useful results to the extent discussed herein.

For **2** (R = Me), a red plate crystal from C₆H₆/MeOH was used for data collection. Three representative reflections measured at 60 min intervals remained constant, and no decay corrections were applied. All four ethoxy groups of the dithiophosphate ligands had high thermal motions indicating possible disorder; a suitable model of the disorder could not be refined, and a single set of ethoxy groups was utilized.

For **3** (R = Me) CF₃SO₃⁻, an orange block crystal from CH₂-Cl₂/Et₂O was used. Three representative reflections measured every 60 min varied 2.6% over the course of data collection, and a linear correction was applied. Several carbon atoms of the dithiophosphate ligands were disordered: C(17) was modeled as two half-occupancy atoms; C(23)–C(24) was modeled as two ethyl groups in a 2:1 ratio. The CF₃SO₃⁻ anion was rotationally and positionally disordered; this was modeled as a single carbon with three F₃ groups and two sulfur positions with oxygen complements.

For **4** (R = Et), an orange-yellow block crystal from CDCl₃/EtOH was used. Three representative reflections measured every 60 min decreased 1.8% during data collection, and a linear correction was applied. A secondary extinction correction was also applied. The compound was a solvate with 0.83 CDCl₃. The chlorines of the CDCl₃ were disordered and were modeled as three sets of 33%, 33%, and 17% occupancies; the D atom was not included in the structure. Two ethoxy and one ethyl portion of the dithiophosphate ligands were also disordered and were modeled as follows: O(3)–C(17)–C(18) was modeled as two half-occupancy groups; O(4)–C(19)–C(20) was modeled as two groups in a 2:1 ratio; and C(21)–C(22) was modeled as two groups in a 3:1 ratio.

Selected results are listed in Tables 2 and 3, while the structures are shown in Figures 1–3.

Results

For simplicity, abbreviations are used as follows. The abbreviations for organic groups are footnoted.³⁰ The bracket abbreviation {Mo₂} denotes the bis(tolylimido)–bis(diethyl dithiophosphato)–μ-acetato–dimolybdenum portion, {Mo₂–(NT_o)₂(S₂P(OEt)₂)₂(μ–O₂CMe)}³⁺. The bracket portion omits the bridge sulfides and thiolates; these groups are identified as a prefix and suffix to the {Mo₂} term. In this manner the dimer anion **1** with two bridge sulfides is indicated as S{Mo₂}S⁻; the μ-thiolate–μ-sulfide complexes **2** are indicated as RS{Mo₂}S; and the bis-μ-thiolate cations **3** are indicated as RS{Mo₂}SR⁺. When a monoethyl dithiophosphate ligand is present instead of

Table 2. Selected Bond Lengths and Distances (Å)

	2	3	4
Mo(1)–Mo(2)	2.8347(5)	2.878(1)	2.8948(9)
Mo(1)–S(1)	2.431(1)	2.439(2)	2.437(2)
Mo(1)–S(2)	2.354(1)	2.438(2)	2.434(2)
Mo(1)–S(3)	2.525(1)	2.489(3)	2.510(2)
Mo(1)–S(4)	2.552(1)	2.498(3)	2.516(2)
Mo(1)–O(1)	2.192(3)	2.164(5)	2.155(4)
Mo(1)–N(1)	1.731(3)	1.724(6)	1.718(5)
Mo(2)–S(1)	2.439(1)	2.424(2)	2.442(2)
Mo(2)–S(2)	2.356(1)	2.432(2)	2.437(2)
Mo(2)–S(5)	2.514(1)	2.491(3)	2.464(2)
Mo(2)–S(6)	2.560(1)	2.501(3)	2.465(2)
Mo(2)–O(2)	2.204(3)	2.157(6)	2.186(2)
Mo(2)–N(2)	1.730(3)	1.721(7)	1.733(5)
S(1)···S(2)	3.860(2)	3.921(4)	3.920(3)
S(1)–C(25)	1.825(4)	1.814(9)	1.829(7)
S(2)–C(26)		1.832(9)	1.813(7)
S(3)–P(1)	2.001(2)	1.999(4)	1.988(3)
S(4)–P(1)	1.974(2)	1.994(4)	2.005(3)
S(5)–P(2)	1.982(2)	1.997(4)	2.040(3)
S(6)–P(2)	1.987(2)	1.995(4)	2.041(3)
O(1)–C(15)	1.254(5)	1.26(1)	1.258(7)
O(2)–C(15)	1.260(5)	1.26(1)	1.252(7)
N(1)–C(1)	1.372(4)	1.382(9)	1.391(7)
N(2)–C(8)	1.374(5)	1.41(1)	1.380(7)
P(1)–O(3)	<i>a</i>	1.560(6)	<i>a</i>
P(1)–O(4)	<i>a</i>	1.556(6)	<i>a</i>
P(2)–O(5)	<i>a</i>	1.562(6)	1.603(5)
P(2)–O(6)	<i>a</i>	1.572(7)	1.472(5)

^a Disordered.

Table 3. Selected Bond Angles (deg)

	2	3	4
S(1)–Mo(1)–S(2)	107.55(4)	107.04(8)	107.16(6)
S(3)–Mo(1)–S(4)	77.84(5)	79.12(8)	78.89(7)
O(1)–Mo(1)–N(1)	174.4(1)	177.3(3)	177.3(2)
S(1)–Mo(2)–S(2)	107.25(4)	107.70(8)	106.93(6)
S(5)–Mo(2)–S(6)	78.12(5)	79.09(9)	79.63(7)
O(2)–Mo(2)–N(2)	173.1(1)	177.8(3)	173.2(2)
Mo(1)–S(1)–Mo(2)	71.19(3)	72.57(7)	72.78(5)
Mo(1)–S(1)–C(25)	112.6(2)	112.5(3)	112.9(2)
Mo(2)–S(1)–C(25)	113.3(2)	112.2(3)	113.1(2)
Mo(1)–S(2)–Mo(2)	74.01(3)	72.46(7)	72.93(5)
Mo(1)–S(2)–C(26)		112.2(3)	113.7(3)
Mo(2)–S(2)–C(26)		112.2(3)	112.9(2)
Mo(1)–N(1)–C(1)	178.3(3)	176.6(6)	173.3(4)
Mo(2)–N(2)–C(8)	176.8(3)	178.7(6)	173.3(4)
S(3)–P(1)–S(4)	106.73(8)	105.4(2)	106.2(1)
S(5)–P(2)–S(6)	107.35(8)	105.6(2)	101.3(1)
O(3)–P(1)–O(4)	<i>a</i>	98.7(4)	<i>a</i>
O(3)–P(1)–S(3)	<i>a</i>	112.5(3)	<i>a</i>
O(3)–P(1)–S(4)	<i>a</i>	112.9(3)	<i>a</i>
O(4)–P(1)–S(3)	<i>a</i>	113.4(3)	<i>a</i>
O(4)–P(1)–S(4)	<i>a</i>	114.3(3)	<i>a</i>
O(5)–P(2)–O(6)	<i>a</i>	98.6(4)	106.4(3)
O(5)–P(2)–S(5)	<i>a</i>	113.0(3)	107.8(2)
O(5)–P(2)–S(6)	<i>a</i>	113.5(3)	108.0(2)
O(6)–P(2)–S(5)	<i>a</i>	112.9(3)	116.7(3)
O(6)–P(2)–S(6)	<i>a</i>	113.5(3)	116.3(3)

^a Disordered.

a diethyl dithiophosphate, its phosphoryl group is incorporated into the bracket term; thus, RS{Mo₂(PO)}SR indicates [Mo₂–(NT_o)₂(S₂P(OEt)₂)(S₂P(O)OEt)(O₂CMe)(SR)₂], **4**, which contains one monoethyl dithiophosphate ligand. Likewise RS{Mo₂(PO)₂}SR⁻ indicates the anionic complex [Mo₂(NT_o)₂–(S₂P(O)OEt)₂(O₂CMe)(SR)₂]⁻, **5**, which contains two monoethyl dithiophosphate ligands. (Structural illustrations for **1**–**3** were given in the Introduction and are shown in eqs 1–4 (Chart 1), along with those for **4** and **5**.) The tolylimido and the acetate ligands are invariant in all complexes herein.

(28) Cromer, D. T.; Waber, J. T. *International Tables for X-Ray Crystallography*; Kynoch Press: Birmingham, England, 1974; Vol. IV, Table 2.2A. Creagh, D. C.; Hubbell, J. H. *International Tables for Crystallography*; Kluwer Academic Publishers: Boston, MA, 1992; Vol. C, Table 4.2.6.8.

(29) Haub, E. K.; Richardson, J. F.; Noble, M. E. *Inorg. Chem.* **1992**, *31*, 4926–4932.

(30) Abbreviations used in this paper: Me, methyl; Et, ethyl; Bu, *n*-butyl; Bz, benzyl; Ph, phenyl; To, *p*-tolyl; PPN⁺, (Ph₃P)₂N⁺.

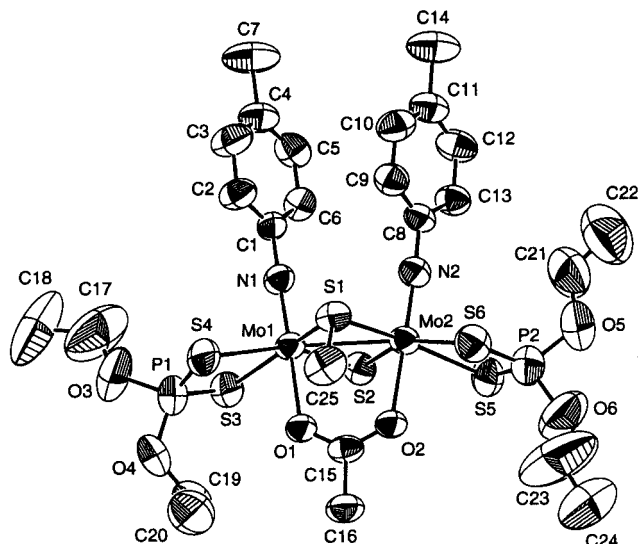


Figure 1. ORTEP view of $\text{MeS}\{\text{Mo}_2\}\text{S}$, **2**.

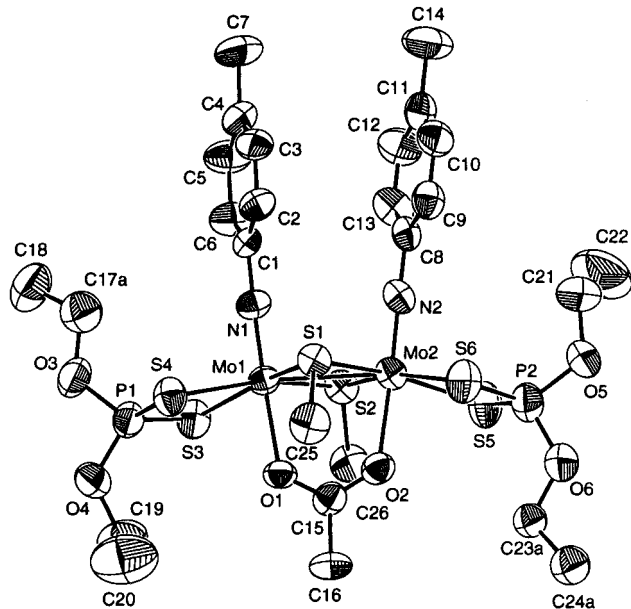


Figure 2. ORTEP view of $\text{MeS}\{\text{Mo}_2\}\text{SMe}^+$, **3**.

The reactions under study constitute a sequential series as given by eqs 1–4. These reactions are described in Part 1. The syntheses and characterizations of several members of the series, including a description of fluxional and nonfluxional isomers, are given in Part 2. Finally, crystallographic studies and structural comparisons are presented for representative members of the sequence in Part 3.

Part 1. The Overall Reaction Series. As noted in the Introduction, the reaction of the dimer anion $\text{S}\{\text{Mo}_2\}\text{S}^-$, **1**, with alkyl halides produces the neutral products $\text{RS}\{\text{Mo}_2\}\text{S}$, **2** (eq 1). This reaction occurs for a variety of substrates including CH_2Cl_2 as previously reported.^{14,15} It is included herein for completeness and for comparison as the first of two sequential alkylation steps.

Alkylation of the second bridge sulfide site produces the bis-thiolate cations $\text{RS}\{\text{Mo}_2\}\text{SR}^+$, **3**, as given by eq 2. With typical alkyl halides, this step is much slower than eq 1 and the two are easily separated.

The $\text{RS}\{\text{Mo}_2\}\text{SR}^+$ cations **3** display two modes of ligand activation. The first is evident in the vulnerability of the bridge thiolate to reattack by nascent halide ion, as given by the

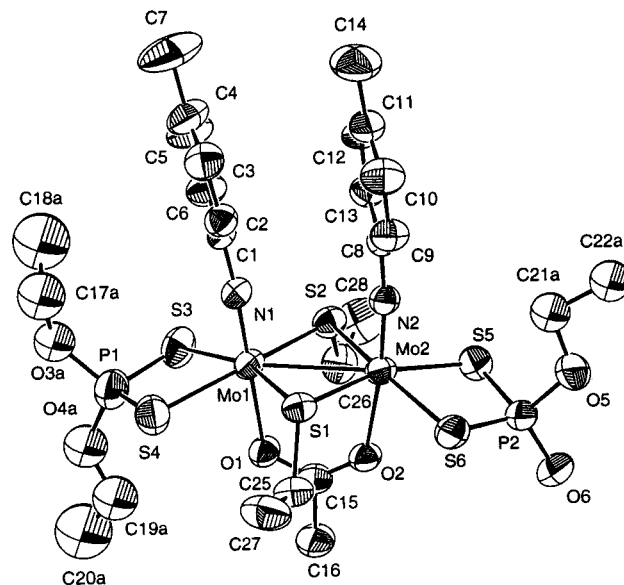


Figure 3. ORTEP view of $\text{EtS}\{\text{Mo}_2(\text{PO})\}\text{SEt}$, **4**.

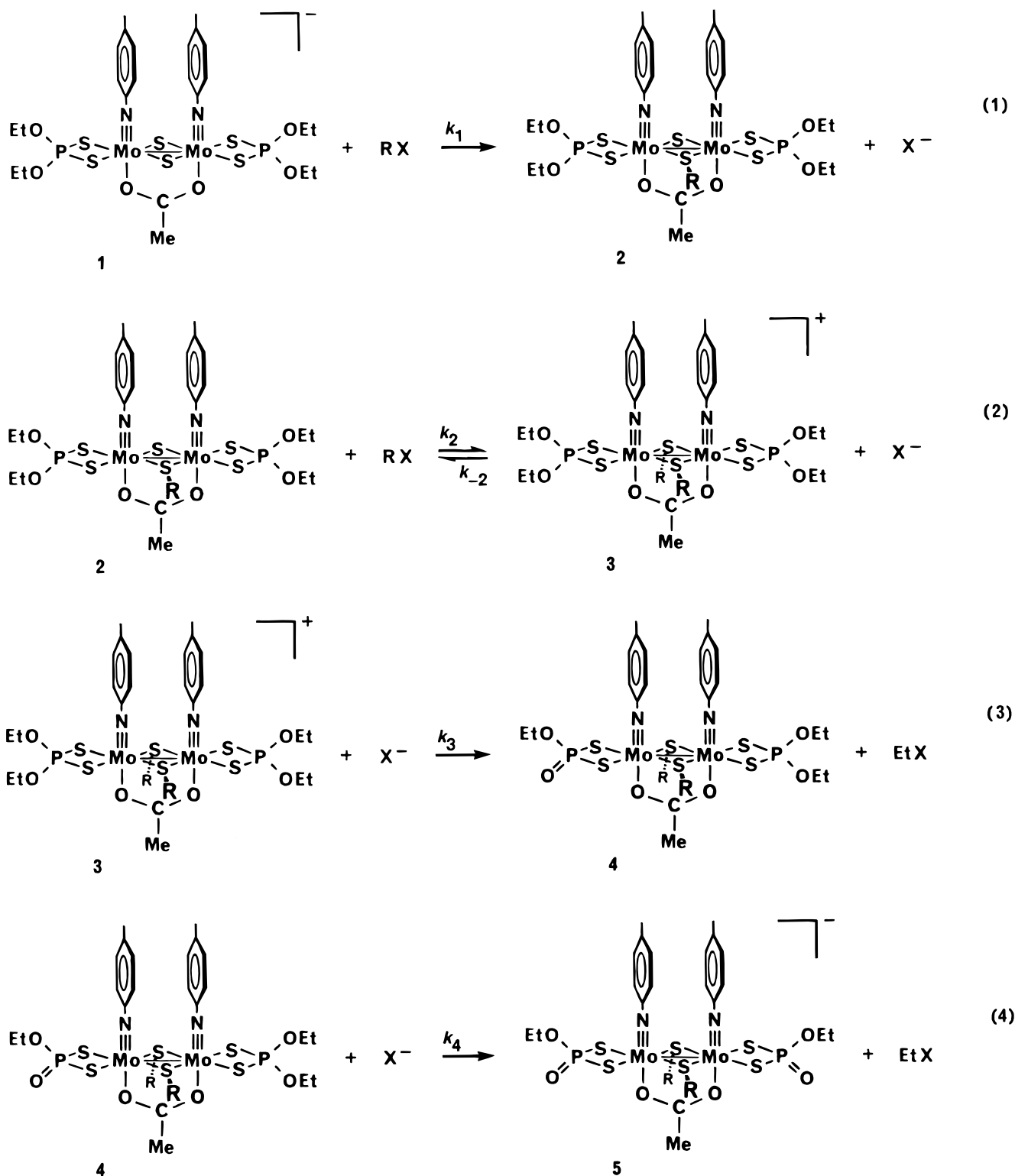
reversibility of eq 2; this dealkylation regenerates neutral $\text{RS}\{\text{Mo}_2\}\text{S}$. The second mode is shown by the facile dealkylation of a diethyl dithiophosphate ligand, eq 3, to produce a neutral complex $\text{RS}\{\text{Mo}_2(\text{PO})\}\text{SR}$, **4** containing both dithiophosphate ligand types, $(\text{EtO})_2\text{PS}_2^-$ and $\text{EtO}(\text{O})\text{PS}_2^{2-}$. The activation is further manifested by de-esterification of the other diethyl dithiophosphate ligand to produce a bis(monoethyl dithiophosphate) anionic complex $\text{RS}\{\text{Mo}_2(\text{PO})_2\}\text{SR}^-$, **5**, in eq 4.

Details of eqs 2–4 follow. Kinetically, some steps were separable depending on conditions. Various reactions were studied using NMR spectroscopy (^{31}P and ^1H) in order to characterize the overall system and to compare the influences of different R groups and nucleophiles. The results which follow describe qualitative trends in rate constants. The emphases are on relative k 's and not overall rates which also include concentrations.

Reactions of $\text{RS}\{\text{Mo}_2\}\text{S}$ with RX . Reactions between $\text{RS}\{\text{Mo}_2\}\text{S}$ **2** and RX in CDCl_3 were studied using variations in both R and X. Comparisons were desired of the equilibrium given by the sulfide alkylation/dealkylation of eq 2, but an actual equilibrium proved unreachable in most cases due to competition between k_{-2} and k_3 . Nevertheless it was possible to evaluate differences in k_2 by using 20-fold RX since this rendered eq 2 (forward) dominant. Even so, it remained necessary to emphasize the earlier stages of the reactions in order to avoid complications from eq 3. Representative percent distributions are shown in Table 4.

The reactions of $\text{BzS}\{\text{Mo}_2\}\text{S}$ **2** with 20-fold benzyl halide clearly revealed the electrophile reactivity sequence $\text{BzI} > \text{BzBr} > \text{BzCl} > \text{BzF}$ for k_2 . With BzI as reactant the amount of the initial product, $\text{BzS}\{\text{Mo}_2\}\text{SBz}^+$ **3**, peaked within minutes while the de-esterification (k_3) occurred slowly. The similarity in the data at 15 and 30 min indicated that an equilibrium position was actually obtained, although by 1 h the execution of eq 3 was becoming significant. With BzBr , the initial reaction (k_2) was much slower; the peak concentration of $\text{BzS}\{\text{Mo}_2\}\text{SBz}^+$ **3** was delayed and a steady state equilibrium was not observed. With BzCl , no reaction was observed through 2 h and only modest ($\sim 5\%$) reaction was seen at 4 h. BzF showed no reaction

Chart 1



through 8 h. The reactivity sequence $\text{BzI} > \text{BzBr} > \text{BzCl} > \text{BzF}$ followed the halides' leaving group abilities.³¹

Comparison was also made using different alkyl groups: reactions of $\text{BzS}\{\text{Mo}_2\}\text{S}$ **2** with 20-fold MeBr and EtBr were conducted and compared to the reaction with BzBr noted above. Representative results are included in Table 4. The data at 15 min showed that initial alkylation (k_2) using MeBr was faster

than that using BzBr . Unfortunately, the initial product $\text{BzS}\{\text{Mo}_2\}\text{SMe}^+$ contained two different thiolate bridges and therefore two separate k_{-2} paths and values. Although the result at 15 min was clear in comparison to the BzBr reaction, the later data were more subject to this complication. For EtBr , no reaction was observed through 2 h. The summary trend was therefore $\text{MeBr} > \text{BzBr} > \text{EtBr}$. The relative celerity of MeBr was a steric result arising from the nearby acetate bridge and also the tolylimido rings when the thiolate group is in the

(31) March, J. *Advanced Organic Chemistry*; John Wiley and Sons: New York, 1992.

Table 4. Percent Distributions for Reactions of $\text{BzS}\{\text{Mo}_2\}\text{S}$ **2** with 20-fold RX in CDCl_3

RX	time	2	\rightleftharpoons	3	\rightarrow	4
BzI	15 min	10		86		4
	30 min	10		84		6
	1.0 h	10		78		12
BzBr	15 min	65		34		<1
	30 min	21		77		2
	1.0 h	11		68		21
BzCl	15 min	100				
	30 min	100				
	1.0 h	100				
BzF	15 min	100				
	30 min	100				
	1.0 h	100				
MeBr	15 min	45		52		3
	30 min	30		62		8
	1.0 h	17		67		16
EtBr	15 min	100				
	30 min	100				
	1.0 h	100				

inverted position (as described in Part 2).²⁹ The classical electronic activation of a benzylic substrate was secondary in this case to steric factors when compared to MeBr, although the electronic aspects did govern the relative outcomes of BzBr and EtBr.

As an additional comparison, it was of interest to examine whether the identity of the preexisting thiolate bridge in $\text{RS}\{\text{Mo}_2\}\text{S}$ had any effect on the rate of alkylation of the sulfide bridge on the opposite side of the dimer. For this purpose, the reaction of 20-fold BzBr with $\text{MeS}\{\text{Mo}_2\}\text{S}$ **2** was compared to the reaction above using $\text{BzS}\{\text{Mo}_2\}\text{S}$. At 15 min, the results showed remaining $\text{MeS}\{\text{Mo}_2\}\text{S}$ **2** (24%) along with the products $\text{MeS}\{\text{Mo}_2\}\text{SBz}^+$ **3** (74%) and $\text{MeS}\{\text{Mo}_2(\text{PO})\}\text{SBz}$ **4** (~2%). Thus, sulfide alkylation was faster for $\text{MeS}\{\text{Mo}_2\}\text{S}$ than for $\text{BzS}\{\text{Mo}_2\}\text{S}$, which demonstrated a cross-core influence of the thiolate on the opposite sulfide's reactivity. The slower reactivity of the former was consistent with benzyl's electron-withdrawing nature relative to methyl's, by both σ and π factors.³²

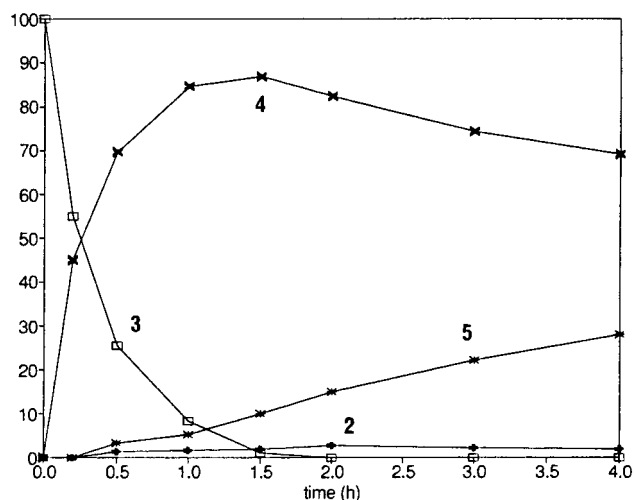
Reactions of $\text{EtS}\{\text{Mo}_2\}\text{SEt}^+$ with Nucleophiles. The reactions above began with $\text{RS}\{\text{Mo}_2\}\text{S}$ **2** and followed k_2 alkylation as the initial step. The series described herein involves the reaction of halide ion with the cation $\text{RS}\{\text{Mo}_2\}\text{SR}^+$ **3**; such reactions could follow either k_{-2} (thiolate dealkylation) or k_3 (phosphoester dealkylation) as the initial step. These were studied using $\text{PPN}^+ \text{X}^-$ and the isolable cation $\text{EtS}\{\text{Mo}_2\}\text{SEt}^+$ (as triflate salt, **3** CF_3SO_3^-). The ethyl derivative of **3** was selected in order to avoid complications from mixed alkyl derivatives; these would otherwise have been possible due to the production of RX from k_{-2} and the production of EtX from eqs 3 and 4.

A statistical factor is involved in comparing the rates of the dithiophosphate C–O and thiolate C–S heterolyses due to the presence of four phosphoester OEt groups and only two thiolate S–Et groups within the complex. This is further complicated by the fact that the OEt groups within each dithiophosphate ligand are chemically inequivalent; thus the four phosphoester groups in the complex are subdivided into two pairs kinetically. This phosphoester distinction is described more fully in Part 2 when the isomers are discussed. For the present comparisons, the results are clearly beyond statistical factors.

Early in these reaction studies, it was realized that CDCl_3 reactions were very slow thereby dictating a change to d_6 -acetone as solvent. For comparison, the reaction of 50 mM $\text{EtS}\{\text{Mo}_2\}\text{SEt}^+$

Table 5. Percent Distributions for Reactions of $\text{EtS}\{\text{Mo}_2\}\text{SEt}^+$ **3** with 3-fold X^- in $(\text{CD}_3)_2\text{CO}$

X^-	time, h	2	\rightleftharpoons	3 (start)	\rightarrow	4	\rightarrow	5	
Cl^-	0.0	0		100		0		0	
	0.5	1		4		82		13	
	1.0	1		0		74		25	
	1.5	2		0		65		33	
	2.0	1		0		56		43	
	3.0	1		0		47		53	
	4.0	2		0		37		61	
	Br^-	0.0	0		100		0		0
		0.5	1		26		70		3
1.0		2		8		85		5	
1.5		2		1		87		10	
2.0		3		0		82		15	
3.0		2		0		75		22	
4.0		2		0		69		28	
I^-		0.0	0		100		0		0
		0.5	2		74		24		0
	1.0	2		55		42		0	
	1.5	4		44		53		0	
	2.0	4		33		63		0	
	3.0	5		20		73		1	
	4.0	5		13		79		2	

**Figure 4.** Percent distribution results for the reaction of $\text{EtS}\{\text{Mo}_2\}\text{SEt}^+$ **3** with Br^- . The curve numbers correspond to compounds **2–5**.

$\{\text{Mo}_2\}\text{SEt}^+$ with 2-fold $\text{PPN}^+ \text{Br}^-$ in CDCl_3 gave only 12% reaction after 80 min; $\text{EtS}\{\text{Mo}_2(\text{PO})\}\text{SEt}$ **4** (k_3 product) was the only product. In d_6 -acetone after 60 min, the reaction yielded 76% $\text{EtS}\{\text{Mo}_2(\text{PO})\}\text{SEt}$ **4** (k_3 product), 8% $\text{EtS}\{\text{Mo}_2(\text{PO})_2\}\text{SEt}^-$ **5** (k_4 product), and 2% $\text{EtS}\{\text{Mo}_2\}\text{S}$ **2** (k_{-2} product).

The effects of variations in X^- were studied with 10 mM $\text{EtS}\{\text{Mo}_2\}\text{SEt}^+$ and 3-fold $\text{PPN}^+ \text{X}^-$ using NMR spectroscopy. Representative percent distributions are listed in Table 5; Figure 4 shows a graphical representation for the reaction using bromide.

The results showed that ester dealkylation (k_3) was much faster than thiolate dealkylation (k_{-2}). In addition, the nucleophilicity sequence $\text{Cl}^- > \text{Br}^- > \text{I}^-$ was obtained for the deesterification (k_3) process. This sequence was evident from the sum of the products $\text{EtS}\{\text{Mo}_2(\text{PO})\}\text{SEt}$ **4** + $\text{EtS}\{\text{Mo}_2(\text{PO})_2\}\text{SEt}^-$ **5**. (The latter is included since it is a $k_3 + k_4$ product.) For example, the sum of **4** + **5** at 0.5 h was 95% for Cl^- , 73% for Br^- , and only 24% for I^- . Unfortunately for the thiolate dealkylation k_{-2} , the speed of k_3 impeded clear comparisons. Furthermore, the k_{-2} product, $\text{EtS}\{\text{Mo}_2\}\text{S}$ **2**, was typically $\leq 3\%$ except when using iodide, and these amounts are prone to large relative integration errors in the NMR spectra. Although the data suggested a modest trend of $\text{I}^- > \text{Br}^- > \text{Cl}^-$ for k_{-2} , that

conclusion was imprudent since the concentrations of remaining **3** followed the same trend and thereby contributed to the overall rates.

In addition to products **2**, **4**, and **5** in these reactions, other compounds become evident at much later stages. At 8.0 h these reached 5% using Cl^- , 3% using Br^- , and 1% using I^- . These compounds were seen as several peaks in the ^{31}P NMR spectra in the 66–72 ppm range, but they were never identified. The various peaks may have been isomers of a single compound. With the use of ^1H coupling, the ^{31}P NMR spectrum showed the unknown peaks as triplets; thus, the dithiophosphate ligands in these compounds were yet monoethyl esters.

As a final note, the reaction of $\text{EtS}\{\text{Mo}_2\}\text{SEt}^+$ **3** was studied with free $(\text{EtO})_2\text{PS}_2^-$ (as Et_3NH^+ salt) as the nucleophile. The reaction was somewhat slow, giving 58% $\text{EtS}\{\text{Mo}_2(\text{PO})\}\text{SEt}$ **4** and 4% $\text{EtS}\{\text{Mo}_2(\text{PO})_2\}\text{SEt}^-$ **5** at 4.0 h. Some of the slowness was indubitably due to the use of a protic acid–base salt which decreased the effective concentration of the $(\text{EtO})_2\text{PS}_2^-$ anion. The triester, $(\text{EtO})_2(\text{EtS})\text{PS}$, was identified in the ^{31}P and ^1H NMR spectra.

Other Reactions. In contrast to the facile reaction of the cation $\text{EtS}\{\text{Mo}_2\}\text{SEt}^+$ **3** with ionic halides, the analogous reaction using neutral $\text{EtS}\{\text{Mo}_2\}\text{S}$ **2** was notoriously slow. This reaction was studied using 3-fold $\text{PPN}^+ \text{Br}^-$ in d_6 -acetone and compared to the result for $\text{EtS}\{\text{Mo}_2\}\text{SEt}^+$ above. After 48 h, only 7% $\text{EtS}\{\text{Mo}_2\}\text{S}$ had reacted compared to 45% for $\text{EtS}\{\text{Mo}_2\}\text{SEt}^+$ in only 0.2 h, corresponding to a >1500-fold difference. The ^{31}P NMR spectrum showed the product as four peaks in the 117.7–118.1 ppm region and four peaks in the 80.3–80.9 ppm region; these sets integrated identically. This pattern indicated that a single phosphoester C–O heterolysis had occurred to give $\text{EtS}\{\text{Mo}_2(\text{PO})\}\text{S}^-$. The ^1H NMR spectrum was consistent with this conclusion and also showed EtBr in a corresponding amount. There was no evidence of any $\text{S}\{\text{Mo}_2\}\text{S}^-$ **1** resulting from thiolate C–S heterolysis. These results confirmed the lack of reversibility in eq 1 and also confirmed the relative inertness of neutral $\text{RS}\{\text{Mo}_2\}\text{S}$ **2** compared to the activated cation $\text{RS}\{\text{Mo}_2\}\text{SR}^+$ **3**.

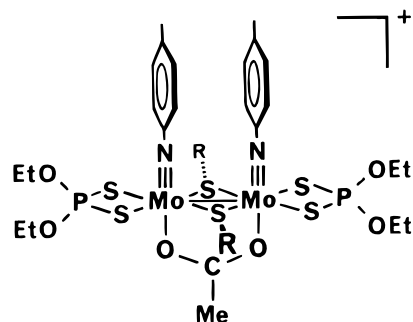
The reversibility of dithiophosphate dealkylation was also investigated. Treatment of anionic $\text{EtS}\{\text{Mo}_2(\text{PO})_2\}\text{SEt}^-$ **5** (as Bu_4P^+ salt) with 10-fold MeI in CDCl_3 and in d_6 -acetone gave a very slow reaction with the majority unreacted after 1 day; NMR spectra revealed broad, unidentifiable peaks with no evidence of phosphoryl methylation. The reaction using $\text{CF}_3\text{SO}_3\text{Me}$ as electrophile, however, was rapid (<10 min in CDCl_3) and provided clear proof of phosphoryl methylation. The ^{31}P NMR spectrum revealed peaks appropriate for the mixed-ester version of $\text{EtS}\{\text{Mo}_2(\text{PO})\}\text{SEt}$ **4** and of a small amount of analogous $\text{EtS}\{\text{Mo}_2\}\text{SEt}^+$ **3**. (The mixed-ester versions contained $(\text{MeO})(\text{EtO})\text{PS}_2^-$ in lieu of $(\text{EtO})_2\text{PS}_2^-$.) The ^1H NMR was definitive by revealing a POCH_3 doublet at 3.75 ppm for the majority product. Thus, under forcing conditions, phosphoryl methylation could be obtained but eq 4 remained effectively irreversible within the overall scheme employing alkyl halide.

The basicity of the monoethyl dithiophosphate ligand was also a matter of interest. This was studied by treating $\text{Bu}_4\text{P}^+ \text{EtS}\{\text{Mo}_2(\text{PO})_2\}\text{SEt}^-$ **5** with increasing amounts of $\text{HBF}_4 \cdot \text{Et}_2\text{O}$ in CDCl_3 . The initial ^{31}P NMR spectrum showed the anion as two overlapping isomer peaks at 80.2 (minor) and 80.0 ppm (major) with a line width of 4.3 Hz for the latter. At 0.6 equiv (per mol of **5**) of acid, one very broad envelope (line width, ~300 Hz) was observed at 89.4 ppm. This indicated a very fast, first protonation equilibrium. At 1.1 equiv of HBF_4 , very broad bands remained between 93 and 98 ppm (86%), and

additional broad bands appeared in the 106–109 ppm range (14%). The latter intensified and sharpened with higher acid amounts: at 3.1 equiv, broad peaks at 107.5 (11%) and 104.3 ppm (73%, line width 25 Hz) dominated and were attributable to the second protonation equilibrium. 2,6-Lutidine (4.0 equiv) was then added, giving several peaks in the 85–86 ppm range (85.8 ppm dominant, 4.3 Hz line width). Further base (40 equiv total) gave no change, indicating that total deprotonation of the complex was obtained with only 4.0 equiv. This implied that 2,6-lutidine was a significantly stronger base than **5**. The sample was extracted with H_2O and dried (MgSO_4). The ^{31}P NMR spectrum showed six peaks between 80 and 81 ppm; the dominant peaks therein and in the ^1H NMR spectrum were only slightly shifted from the initial (preacidification) spectrum. Some of the new peaks were ascribable to isomers of the dithiophosphate (as described in Part 2), but some peaks may have been decomposition (estimated <10%). Thus, although the integrity of the complex as a whole may have been sacrificed to some extent, after acidification and neutralization all dithiophosphates remained ligating. Furthermore, these remained monoesters as shown by a final ^1H -coupled ^{31}P NMR spectrum.

Part 2. Syntheses and Characterizations. Throughout the course of the reactions described above, the spectral identifications of $\text{RS}\{\text{Mo}_2\}\text{SR}^+$ **3**, $\text{RS}\{\text{Mo}_2(\text{PO})\}\text{SR}$ **4**, and $\text{RS}\{\text{Mo}_2(\text{PO})_2\}\text{SR}^-$ **5** were definitive by comparison to spectra of isolated samples. Synthetic methods for one or more members of each type were developed, and the isolated compounds were characterized by ^1H and ^{31}P NMR spectroscopy; some were also confirmed by elemental analyses and by X-ray crystallography as given in Part 3.

The cation complexes $\text{RS}\{\text{Mo}_2\}\text{SR}^+$ (R = Me, Et) were prepared and characterized from the reaction of $\text{RS}\{\text{Mo}_2\}\text{S}$ **2** with alkyl triflates. The synthetic route utilized k_2 of eq 2, and the poor nucleophilicity of CF_3SO_3^- disabled the k_{-2} and k_3 pathways. The two derivatives $\text{MeS}\{\text{Mo}_2\}\text{SMe}^+ \text{CF}_3\text{SO}_3^-$ and $\text{EtS}\{\text{Mo}_2\}\text{SEt}^+ \text{CF}_3\text{SO}_3^-$ were thus obtainable in >90% yields. The solution NMR spectra showed isomers corresponding to inversion of the pyramidal thiolate–sulfur bridges. As previously documented for $\text{RS}\{\text{Mo}_2\}\text{S}$ **2** and related derivatives,^{14–17,29} these are freely fluxional invertomers; they are labeled distal (*d*) or proximal (*p*) depending on the thiolate orientation with respect to the tolylimido rings. For $\text{MeS}\{\text{Mo}_2\}\text{SMe}^+$, the dominant solution isomer contains both thiolate groups in distal orientation (distal–distal, *d-d*); this isomer is portrayed in the prior structural illustrations for **3**. The secondary isomer is distal–proximal (*d-p*); this isomer is shown below for comparison.



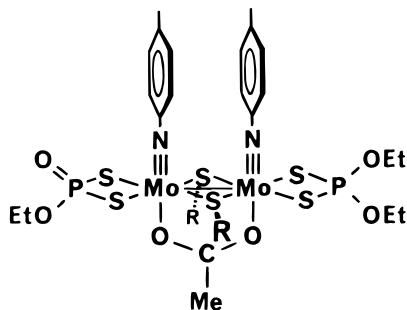
The ratio (*d-d:d-p*) is 3.1. For $\text{EtS}\{\text{Mo}_2\}\text{SEt}^+$, the *d-d* and *d-p* isomers are again obtained but in nearly equal amounts with a ratio of 0.95. Neither compound showed evidence for the proximal–proximal (*p-p*) isomer. The invertomer distributions are nonstatistical with a clear distal preference. Structural and

electronic differences between distal and proximal invertomers have been previously discussed for several $ZS\{Mo_2\}S$ compounds.²⁹

Infrared spectra of the two $RS\{Mo_2\}SR^+ CF_3SO_3^-$ ($R = Me, Et$) compounds were similar. Except for triflate absorptions, these spectra were much like the infrared spectra of the previously characterized derivatives $RS\{Mo_2\}S$.

The crystal structure of $MeS\{Mo_2\}SMe^+ CF_3SO_3^-$ was also obtained, confirming the spectroscopic identification; the structure is described in Part 3.

Synthesis and isolation of the singly de-esterified complexes $RS\{Mo_2(PO)\}SR$ **4** proved very tedious, partly due to their middle role in a multistep sequence and also due to the presence of more isomers. These compounds were isolated for $R = Et$ and Bz in modest yields, 24% and 34%. The additional isomers arise from the orientation of the phosphoryl linkage, which can also be described as distal or proximal with respect to the tolylimido rings. Unlike the bridge sulfur invertomers which are freely fluxional, the monoethyl dithiophosphate ligands are locked configurationally; no fluxionality was observed over 8 days in solution for these ligands. For purposes of distinction in the current descriptions of the different isomers, the distal and proximal labels are combined with *S* (for bridge *SR*) and *P* (for $P=O$). The prior structural illustrations for **4** portrayed the *S/d-d*, *P/d* isomer. The *S/d-d*, *P/p* isomer is shown below as another example.



Combining all phosphoryl and thiolate orientational options, six unique isomers were possible. The synthetic procedure for $EtS\{Mo_2(PO)\}SEt$ yielded a product with a single *P* isomer; the procedure for $BzS\{Mo_2(PO)\}SBz$ gave a product which appeared to contain a second *P* isomer in a small amount. Both of the isolated compounds showed the *S/d-d* and *S/d-p* invertomers in solution. During the course of studies of the reactions between $EtS\{Mo_2\}SEt^+$ and halide described in Part 1, four isomers were spectroscopically observed corresponding to all four possible permutations involving the pairs *S/d-d* vs *S/d-p* and *P/d* vs *P/p*. The *S/p-p* isomer was never seen in any case.

NMR spectra of the isolated compounds were complex although the two types of dithiophosphate ligands were clearly resolved. The ^{31}P NMR spectra showed the $(EtO)_2PS_2^-$ ligand at 112 ppm and the $EtO(O)PS_2^{2-}$ ligand at 77 ppm. The 1H NMR spectra showed upfield peaks for the ethyl group of $EtO(O)PS_2^{2-}$, relative to those of $(EtO)_2PS_2^-$. The low symmetry of the compounds was especially evident in the 1H NMR spectra. Even the CH_2 protons within a single bridge thiolate were no longer equivalent and the SCH_2 protons were geminally coupled to each other.

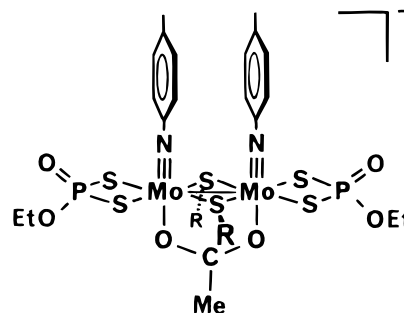
A 1D-ROESY experiment was conducted for $EtS\{Mo_2(PO)\}SEt$ in an effort to determine the phosphoryl orientation of the isolated product. Use was made of the $(EtO)_2PS_2^-$ ligand for internal comparison: irradiation of tolylimido ring protons gave a significant enhancement of one methylene group of this

$(EtO)_2PS_2^-$ ligand, identifying that CH_2 as the one nearer the ring. The effect was similar for the methylene group of $EtO(O)PS_2^-$, indicating that the ethyl of that ligand was also near the ring; this meant that the $P=O$ linkage was distal for the isolated product.

The crystal structure of $EtS\{Mo_2(PO)\}SEt$ is described in Part 3 and fully confirms the spectroscopic identification.

The doubly de-esterified anion complexes $RS\{Mo_2(PO)_2\}SR^-$, **5**, were prepared and characterized for $R = Et$. The synthesis involved the reaction of excess chloride ion with $EtS\{Mo_2\}SEt^+ CF_3SO_3^-$ thereby directly executing eqs 3 and 4. Although the reaction studies described in Part 1 had used PPN^+ salts, clean isolation of the anion complex $EtS\{Mo_2(PO)_2\}SEt^-$ was not achieved with this cation. The use of Bu_4P^+ did allow for isolation in modest yield and fortuitously of a single phosphoryl isomer. Spectroscopically, the PPN^+ and Bu_4P^+ products were virtually identical with only slight differences in chemical shifts for the anion portion in the ^{31}P NMR spectra.

For $EtS\{Mo_2(PO)_2\}SEt^-$, nine unique isomers were possible for the various combinations of phosphoryl and thiolate orientations. The synthetic product $Bu_4P^+ EtS\{Mo_2(PO)_2\}SEt^-$ contained both phosphoryl groups in distal orientation, *P/d-d*; in solution, this product also gave *S/d-d* and *S/d-p* invertomers. The former, depicted in the prior structural diagrams for **5**, was the major isomer (invertomer ratio, 2.7). Another phosphoryl isomer, *P/p-p*, is illustrated below for comparison.



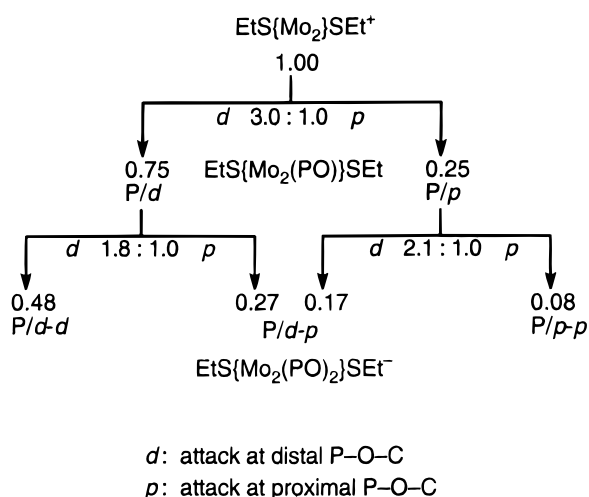
The IR spectrum of the solid product showed an intense phosphoryl stretch at 1204 cm^{-1} . Notably, the classical, very intense absorptions in the $950\text{--}1080\text{ cm}^{-1}$ region, which so typify $(EtO)_2PS_2$ derivatives and which have long been debated as related to $P-O-C$ modes,^{33,34} were replaced by a single peak at 1048 cm^{-1} of only moderate intensity.

Although not present in the isolated product $Bu_4P^+ EtS\{Mo_2(PO)_2\}SEt^-$, all of the permutations of the two phosphoryl linkages (*P/d-d*, *P/d-p*, and *P/p-p*) were observed in some crude product preparations and in various reactions described in Part 1. Combining those reaction studies with the characterization of the *P* isomers in the isolated products $EtS\{Mo_2(PO)\}SEt$ **4** and $EtS\{Mo_2(PO)_2\}SEt^-$ **5**, it was possible to trace the relative production of each phosphoryl isomer through the sequence of eqs 3 and 4. The results are given in Scheme 1 for one reaction sequence between $EtS\{Mo_2\}SEt^+ CF_3SO_3^-$ and $PPN^+ Cl^-$ in d_6 -acetone. The kinetic inequivalence of the phosphoester groups is clearly evident: dealkylation is faster (two- to threefold) at the distal ester positions. The slower proximal reactivity is understandable in light of steric limitations imposed by the nearby tolylimido rings.

(33) Thomas, L. C. *Interpretation of the Infrared Spectra of Organophosphorus Compounds*; Heyden: London, 1974.

(34) Corbridge, D. E. C. *Topics in Phosphorus Chemistry*; Interscience: New York, 1969; Vol. 6, pp 235–365.

Scheme 1



Part 3. Structural Studies. Three crystal structures are presented. The structures of $\text{MeS}\{\text{Mo}_2\}\text{S}$ **2** and of $\text{MeS}\{\text{Mo}_2\}\text{SMe}^+ \text{CF}_3\text{SO}_3^-$ **3** were compared in an effort to determine structural evidence within the latter for the thiolate and dithiophosphate ligand activation. The third crystal structure was for $\text{EtS}\{\text{Mo}_2(\text{PO})\}\text{SEt}$ **4**. This was obtained to compare the structural differences, within that single compound, between a monoanionic diester $(\text{EtO})_2\text{PS}_2^-$ and a dianionic monoester $(\text{EtO})\text{OPS}_2^{2-}$ unit; in addition, the structure was of interest as a rare example of monoalkyl dithiophosphate complexes.

The structures are shown in Figures 1–3. Selected metrical results are listed in Tables 2 and 3.

The structure of $\text{MeS}\{\text{Mo}_2\}\text{S}$ (Figure 1) is similar to those of various $\text{ZS}\{\text{Mo}_2\}\text{S}$ compounds reported previously including $\text{EtSS}\{\text{Mo}_2\}\text{S}$,³⁵ $\text{H}_2\text{NS}\{\text{Mo}_2\}\text{S}$,²⁹ $\text{Me}_3\text{CCH}=\text{NS}\{\text{Mo}_2\}\text{S}$,²⁹ and $\text{BzS}\{\text{Mo}_2\}\text{S}$.¹⁷ Several common features of this group are as follows. The overall structures are idealized C_s symmetry with a vertical mirror plane bisecting the SMo_2S core and containing the sulfur bridges. Imido linkages are linear, and acetate ligands bridge symmetrically. The SMo_2S cores are virtually planar; for the present $\text{MeS}\{\text{Mo}_2\}\text{S}$ the dihedral angle for MoS_2 planes is indeed $180.0(1)^\circ$. $\text{Mo}-\text{S}(\text{bridge})$ bonds to tricoordinate $\text{S}(1)$ are longer than those to sulfide $\text{S}(2)$ corresponding to greater π bonding within the $\text{Mo}-\text{S}(2)$ bonds.²⁹ For $\text{MeS}\{\text{Mo}_2\}\text{S}$, $\text{Mo}-\text{S}(1)$ bond lengths are 2.431(1) and 2.439(1) Å vs 2.354(1) and 2.356(1) Å for those of $\text{Mo}-\text{S}(2)$. Due to the disparate $\text{Mo}-\text{S}(\text{bridge})$ bonds, $\text{Mo}-\text{S}(\text{dithiophosphate})$ bond lengths are also different; these inversely correlate with trans $\text{Mo}-\text{S}(\text{bridge})$ bond lengths and reflect the greater trans influence of sulfide $\text{S}(2)$ compared to thiolate $\text{S}(1)$. The shorter $\text{Mo}-\text{S}(\text{dithiophosphate})$ bond lengths are 2.525(1) and 2.514(1) Å for those trans to thiolate $\text{S}(1)$, while the longer bond lengths are 2.552(1) and 2.560(1) Å for those trans to sulfide $\text{S}(2)$.

Compared to the previously characterized benzyl thiolate $\text{BzS}\{\text{Mo}_2\}\text{S}$ structure,¹⁷ the structure of $\text{MeS}\{\text{Mo}_2\}\text{S}$ differs significantly in one aspect which is important to the present study: the bridge thiolate $\text{S}(1)-\text{C}(25)$ bond length is 1.825(4) Å in $\text{MeS}\{\text{Mo}_2\}\text{S}$, but it was 1.852(6) Å in $\text{BzS}\{\text{Mo}_2\}\text{S}$.

The structure of the activated cation $\text{MeS}\{\text{Mo}_2\}\text{SMe}^+ \text{CF}_3\text{SO}_3^-$ is now described and compared to that of inert, neutral $\text{MeS}\{\text{Mo}_2\}\text{S}$. Conversion of the $\text{S}(2)$ sulfide in the latter to a second thiolate in the former removes the inequivalence of the bridge sulfurs and yields idealized C_{2v} symmetry within the

cation. All $\text{Mo}-\text{S}(\text{thiolate})$ bonds are now equivalent, and their lengths (2.424(2)–2.439(2) Å) are similar to those in $\text{MeS}\{\text{Mo}_2\}\text{S}$ (2.431(1) and 2.439(1) Å).

The reduced donation by the second thiolate bridge in $\text{MeS}\{\text{Mo}_2\}\text{SMe}^+$ compared to the sulfide bridge in $\text{MeS}\{\text{Mo}_2\}\text{S}$ is manifested in a number of ways. The central SMo_2S core is expanded with a longer $\text{Mo}-\text{Mo}$ bond (2.878(1) vs 2.8347(5) Å) and a greater cross-core $\text{S}(1)\cdots\text{S}(2)$ distance (3.921(4) vs 3.860(2) Å). The core remains fairly planar, with a dihedral angle between MoS_2 planes of $174.3(1)^\circ$. Some coligands also respond. The acetate bridge and the dithiophosphate ligands contract toward the metals. $\text{Mo}-\text{O}$ bonds are substantially shortened (2.157(6) and 2.164(5) Å vs 2.192(3) and 2.204(3) Å). $\text{Mo}-\text{S}(\text{dithiophosphate})$ bonds (2.489(3)–2.501(3) Å) are shorter than the corresponding bonds in $\text{MeS}\{\text{Mo}_2\}\text{S}$ (trans to thiolate, 2.514(1) and 2.525(1) Å). The $\text{Mo}-\text{N}(\text{imido})$ bonds, however, are not significantly affected (1.721(7) and 1.724(6) Å vs 1.730(3) and 1.731(3) Å).

The methyl thiolate ligands are identical in the two compounds. All methyl groups are in distal invertomer positions, consistent with the major solution isomer for both compounds. $\text{S}-\text{C}$ bond lengths are similar (1.814(9) and 1.832(9) Å vs 1.825(4) Å). Even the pyramidity of the thiolate sulfur bridges is similar, as judged by the sum of the bond angles at the sulfur sites ($297.3(8)^\circ$ and $296.9(8)^\circ$ vs $297.1(4)^\circ$). Thus, the activation of the MeS bridge to nucleophilic attack is not evidenced in the structural data by any $\text{Mo}/\text{S}/\text{C}$ bond parameters.

Structural evidence for the activation of the dithiophosphates is limited to the $\text{Mo}-\text{S}(\text{dithiophosphate})$ contraction as noted above. $\text{P}-\text{S}$ bond lengths are similar in the two compounds. Beyond the P atoms the structure for $\text{MeS}\{\text{Mo}_2\}\text{S}$ was subject to disorder, and further comparisons thereof are precluded.

The structure of $\text{EtS}\{\text{Mo}_2(\text{PO})\}\text{SEt}$ is now described. The complex has idealized C_s symmetry, but now the vertical mirror plane contains the two molybdenums. The critical intramolecular difference lies in the $(\text{EtO})_2\text{PS}_2^-$ ligand on $\text{Mo}(1)$ compared to the dianionic $\text{EtO}(\text{O})\text{PS}_2^{2-}$ ligand on $\text{Mo}(2)$.

The $\text{Mo}-\text{Mo}$ bond is barely longer, 2.8948(9) Å, and the cross-core $\text{S}(1)\cdots\text{S}(2)$ distance (3.920(3) Å) is identical to the corresponding parameters of $\text{MeS}\{\text{Mo}_2\}\text{SMe}^+$. Despite the formal inequivalence, the $\text{Mo}-\text{S}(\text{thiolate})$ bond lengths are all similar (2.434(2)–2.442(2) Å), and these are comparable to the corresponding $\text{Mo}-\text{S}(\text{thiolate})$ bonds in both $\text{MeS}\{\text{Mo}_2\}\text{S}$ and $\text{MeS}\{\text{Mo}_2\}\text{SMe}^+$ (2.424(2)–2.439(2) Å).

The acetate no longer binds symmetrically, reflecting the disparity in the dithiophosphate donors. The $\text{Mo}(1)-\text{O}(1)$ bond length is 2.155(4) Å compared to 2.186(2) Å for $\text{Mo}(2)-\text{O}(2)$. Since $\text{Mo}(2)$ possesses doubly negative $\text{EtO}(\text{O})\text{PS}_2^{2-}$, the longer $\text{Mo}(2)-\text{O}(2)$ bond is consistent with less electron demand by $\text{Mo}(2)$ than by $\text{Mo}(1)$. The $\text{Mo}(1)-\text{O}(1)$ bond length is contracted to an extent comparable to that noted above in $\text{MeS}\{\text{Mo}_2\}\text{SMe}^+$ (2.157(6) and 2.164(5) Å).

$\text{Mo}-\text{S}(\text{dithiophosphate})$ bonds are shorter for the dinegative $\text{EtO}(\text{O})\text{PS}_2^{2-}$ ligand (2.464(2) and 2.465(2) Å) than for the uninegative $(\text{EtO})_2\text{PS}_2^-$ ligand (2.510(2) and 2.516(2) Å). The latter are typical: these are comparable to those in $\text{MeS}\{\text{Mo}_2\}\text{S}$ which are trans to the thiolate bridge (2.514(1) and 2.525(1) Å). The $\text{Mo}-\text{S}$ bonds to the dinegative ligand, however, are the shortest of all $\text{Mo}-\text{S}(\text{dithiophosphate})$ bonds in the three compounds reported herein, consistent with the greater electron donation from the $\text{EtO}(\text{O})\text{PS}_2^{2-}$ dianion. The corresponding $\text{P}-\text{S}$ bonds follow an inverse trend: the $\text{P}-\text{S}$ bond lengths in the monoanion ligand are typical (1.998(3) and 2.005(3) Å) while those in the dianion ligand are significantly longer (2.040-

(3) and 2.041(3) Å). This is consistent with the relative formal PS bond orders of the free ligands, 1.5 in (EtO)₂PS₂²⁻ vs 1 in EtO(O=)PS₂²⁻.

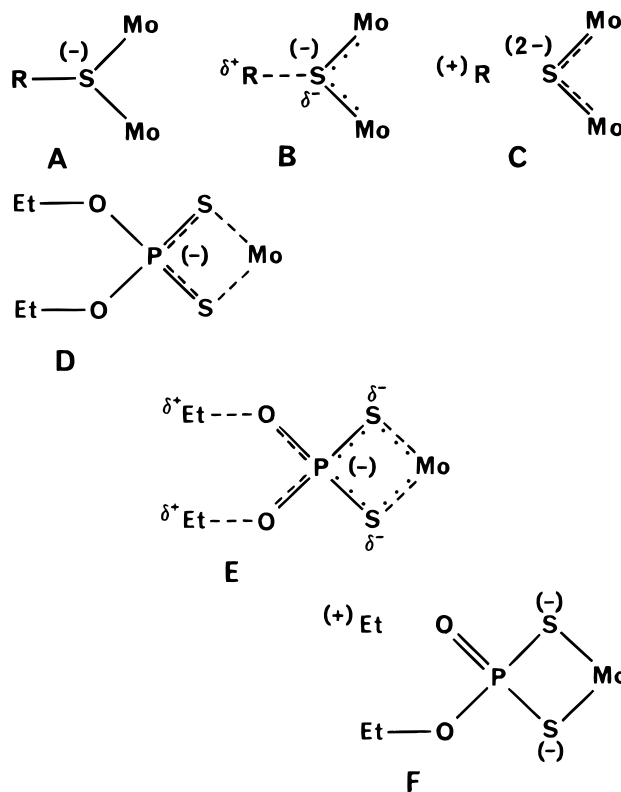
Beyond the P atoms, disorder within the monoanion (EtO)₂PS₂⁻ precludes further comparisons using that ligand. Within the dianionic ligand, the phosphoryl P=O bond is very short (1.472(5) Å) compared to the ester P–O bond (1.603(5) Å). The greater steric effect of P=O vs P–O is evident: of the six tetrahedral angles at P(2), the three angles involving O(6) (i.e., Z–P(2)=O(6) angles) are expanded while the three others (those not involving O(6)) are correspondingly compressed when these are compared to the analogous angles of the (EtO)₂PS₂²⁻ ligands within MeS{Mo₂}SMe⁺ **3**.

Given the paucity of metallocomplexes containing monoester dithiophosphate ligands, brief mention of comparative crystallographic results is appropriate. Only three crystal structure studies could be located, but only one, that of [(Ph₂PC₂H₄AsPh₂)Ni(S₂P(O)OMe)],³⁶ contains the appropriate bidentate RO(O)PS₂²⁻ ligand. The other two include [(NC)₂C₂S₂Ni(S₂P(OH)OEt)]⁻³⁷ which contains a monoanionic, acid ligand, EtO(HO)PS₂⁻, and [(Me₂PhP)₄Re₂N₂(S₂P(O)OEt)₂],³⁸ which contains EtO(O)PS₂²⁻ as a bridging, tridentate (S,S',O) ligand. Restricting therefore to the case of [(Ph₂PC₂H₄AsPh₂)Ni(S₂P(O)OMe)], comparison to the present structure of EtS{Mo₂(PO)}SEt **4** shows the RO(O)PS₂²⁻ ligands to be very similar. Relevant bond lengths from the nickel structure are the following: P=O, 1.47(1) Å; P–O, 1.597(8) Å; and P–S, 2.024(4) and 2.032(4) Å.

Discussion

Two points are immediately notable. First, the cations RS{Mo₂}SR⁺, by themselves, are very unusual in displaying two different types of ligand activation. Second, in comparison to the neutral complexes RS{Mo₂}S, the cations demonstrate the effects of electronic stress and the response of the ligands to that stress. The stress arises directly from the diminution in electron contribution from a sulfur bridge upon alkylation. This renders the molybdenum centers potentially more electron withdrawing toward other ligands. The effect is manifested chemically within the thiolate and dithiophosphate ligands and structurally within metal–ligand bond distances. The decrease in the bridge sulfur contribution is fairly costly to the complex as a whole, since the second dithiophosphate ligand remains activated even after the first is de-esterified.

The activation of the thiolate and dithiophosphoester groups toward heterolysis can be explained using simple inductive arguments, although other effects may also be operating. Given the increase in electron withdrawal, the drift in electron density toward the molybdenums and toward dealkylation can be pictorially represented as shown in A–C for a thiolate and in D–F for a dithiophosphate. (In these diagrams, the different line representations are meant to convey relative bond strength information and are not necessarily formal orders. The parenthetical full charges which are shown are for the ligand.) Variations in the bonding were corroborated in some cases by the crystallographic comparisons. On the basis of the various reactions which were studied, the actual dealkylation steps overall are consistent with S_N2 mechanisms in weakly polar media.



The thiolate dealkylation (*k*₋₂ step) is similar to some other C–S cleavage reactions in metal–thiolate complexes. This general area has been of interest for many years due in part to hydrodesulfurization. In addition, thiolate dealkylations have been used synthetically to prepare metal–sulfide complexes. Of the various metal–thiolate C–S cleavage reactions which have been reported, three general mechanisms are well represented to date:^{39–44} heterolytic (nucleophilic) substitution, alkene elimination, and homolysis. Many reported reactions do not tidily fit these categories, and indubitably other mechanisms avail. For example, SET is a reasonable proposition especially for aryls, although this pathway may be difficult to distinguish from S_H1 in the case of metal thiolates. Nevertheless, SET has been proposed for desulfurizations of condensed thiophenic substrates using nickel complexes.⁴⁵ Heterolytic substitutions, such as those of the present study, are frequently encountered when an additional nucleophile is present in the solution. Among the oldest of these are reactions, some used synthetically, between alkanethiolate sources and metal halide reagents to give metal sulfide products + RX.⁴⁴

(36) Gastaldi, L.; Porta, P.; Tomlinson, A. G. *J. Chem. Soc., Dalton Trans.* **1974**, 1424–1429.

(37) Kirmse, R.; Dietzsch, W.; Stach, J.; Golič, L.; Böttcher, R.; Brunner, W.; Gribnau, M. C. M.; Keijzers, C. P. *Mol. Phys.* **1986**, *57*, 1139–1152.

(38) Abram, U.; Ritter, S. *Inorg. Chim. Acta* **1993**, *210*, 99–105.

(39) The literature is extensive, and only representative examples are cited. General references include the following: Blower, P. J.; Dilworth, J. R. *Coord. Chem. Rev.* **1987**, *76*, 121–185. Dilworth, J. R. *Stud. Inorg. Chem.* **1984**, *5*, 141–165.

(40) Curtis, M. D.; Druker, S. H. *J. Am. Chem. Soc.* **1997**, *119*, 1027–1036. Riaz, U.; Curnow, O. J.; Curtis, M. D. *J. Am. Chem. Soc.* **1994**, *116*, 4357–4363.

(41) Coucouvanis, D.; Hadjikyriacou, R. L.; Kanatzidis, M. G. *Inorg. Chem.* **1994**, *33*, 3645–3655.

(42) Birnbaum, J.; Laurie, J. C. V.; Rakowski DuBois, M. *Organometallics* **1990**, *9*, 156–164. Weberg, R. T.; Laurie, J. C. V.; Rakowski DuBois, M. *J. Coord. Chem.* **1988**, *19*, 39–48. Laurie, J. C. V.; Duncan, L.; Haltiwanger, R. C.; Weberg, R. T.; Rakowski DuBois, M. *J. Am. Chem. Soc.* **1986**, *108*, 6234–6241.

(43) Ng, C. T.; Wang, X.; Luh, T.-Y. *J. Org. Chem.* **1988**, *53*, 2536–2539.

(44) Boorman, P. M.; Patel, V. D. *Inorg. Chim. Acta* **1980**, *44*, L85–L87. Boorman, M. P.; Chivers, T.; Mahadev, K. N.; O'Dell, B. D. *Inorg. Chim. Acta* **1976**, *19*, L35–L37.

(45) Eisch, J. J.; Hallenbeck, L. E.; Han, K. I. *J. Am. Chem. Soc.* **1986**, *108*, 7763–7767.

Although there has been considerable progress in the delineation of the mechanistic aspects of C–S cleavage within metallothiolate complexes, the manner by which thiolate ligands are activated toward cleavage remains an important fundamental. After all, many metallothiolate complexes are very stable. The present work demonstrates inductive activation, which has also been suggested in thioether and related cleavage studies.⁴⁶ In other thioether and thiophenic complexes, a different mode of C–S activation involved electron donation from the metal into C–S σ^* orbitals.^{47,48} This is not significant in the present work due to the lack of adequate metal electrons.

In contrast to thiolate dealkylations, C–O cleavage of phosphoester ligands is much less established despite the avid interest in metal-catalyzed P–O cleavage in biological studies. With specific regard to dithiophosphates, these ligands tend to be fairly inert and few examples of de-esterification have been well characterized. The well-defined examples include as products [(Ph₂PC₂H₄(As,P)Ph₂)Ni(S₂P(O)OMe)],³⁶ [(NC)₂-C₂S₂Ni(S₂P(OH)OEt)][−],³⁷ [(Me₂PhP)₄Re₂N₂(S₂P(O)OEt)₂],³⁸ [(R₃P)₂M(S₂P(O)OR') (M = Pd,⁴⁹ Pt⁵⁰), and [(Ph₂PC₂H₄(As,P)-Ph₂)Co(S₂P(OMe)₂)(S₂P(O)OMe)].⁵¹ Except for [(NC)₂C₂S₂Ni(S₂P(OH)OEt)][−], whose mechanism of formation was not evident, the other products conceivably arose from nucleophilic attack on a bound (RO)₂PS₂[−] ligand. In each of those cases, free (RO)₂PS₂[−] (added in excess or liberated in situ) may have been the nucleophile, although some of the cases also allowed for Cl[−] or phosphine as nucleophile. For [(Ph₂PC₂H₄PPh₂)Co-

(S₂P(OMe)₂)(S₂P(O)OMe)], kinetic results confirmed the mechanism and the triester (MeO)₂(MeS)PS was specifically identified; the reaction involved demethylation of [(Ph₂PC₂H₄PPh₂)Co(S₂P(OMe)₂)₂]⁺ by free (MeO)₂PS₂[−] liberated in a prior step. This was a sterically limited reaction, however: the analogous reaction using the isobutyl ester apparently failed and the stable salt [(Ph₂PC₂H₄PPh₂)Co(S₂P(OCH₂CHMe₂)₂)₂]⁺ (Me₂CHCH₂O)₂-PS₂[−] was isolated.⁵²

The reason for the dithiophosphate ligand to display this vulnerability to de-esterification was not necessarily evident in the reactions cited. The present work was able to demonstrate that the enhanced reactivity was a result of increased electron withdrawal. The present work also showed definitive dealkylation both by X[−] and by (EtO)₂PS₂[−] as given by the observation of EtX and triester (EtO)₂(EtS)PS products.

Once formed, the RO(O)PS₂^{2−} ligand appears to be fairly robust: within the present study, no further dealkylation was ever observed and, for [(Ph₂PC₂H₄AsPh₂)Ni(S₂P(O)OMe)],³⁶ thermal stability was reported to 225 °C whereupon the phosphinoarsine ligand decomposed. The phosphoryl linkage was shown to be poorly nucleophilic and weakly basic in the present work. The donor ability of a phosphoryl oxygen in a dithiophosphate monoester ligand is also evidenced in two of the complexes cited above: [(NC)₂C₂S₂Ni(S₂P(OH)OEt)][−]³⁷ contains the protonated ligand and [(Me₂PhP)₄Re₂N₂(S₂P(O)-OEt)₂]³⁸ involves tridentate (S,S',O) coordination.

Acknowledgment. This work was supported by research awards from the National Science Foundation and the University of Louisville.

Supporting Information Available: Tables of crystal data, atomic coordinates, thermal parameters, bond lengths, and bond angles for **2**, **3** CF₃SO₃[−], and **4**. This material is available free of charge via the Internet at <http://pubs.acs.org>.

IC981303L

(52) Monacelli, F.; Tomlinson, A. A. G. *Gazz. Chim. Ital.* **1980**, *110*, 43–47.

(46) Bernatis, P.; Haltiwanger, R. C.; Rakowski DuBois, M. *Organometallics* **1992**, *11*, 2435–2443.

(47) Bianchini, C.; Meli, A. *Acc. Chem. Res.* **1998**, *31*, 109–116.

(48) Mullen, G. E. D.; Went, M. J.; Wocadlo, S.; Powell, A. K.; Blower, P. J. *Angew. Chem., Int. Ed. Engl.* **1997**, *36*, 1205–1207.

(49) Fackler, J. P., Jr.; Seidel, W. C. *Inorg. Chem.* **1969**, *8*, 1631–1639.

(50) Alison, J. M. C.; Stephenson, T. A. *J. Chem. Soc., Dalton Trans.* **1973**, 254–263. Colton, R.; Stephenson, T. A. *Polyhedron* **1984**, *3*, 231–234.

(51) Borghi, E.; Di Castro, V.; Monacelli, F.; Tomlinson, A. A. G. *J. Chem. Soc., Dalton Trans.* **1978**, 950–955. Tomlinson, A. A. G.; Mattoigno, L.; Di Castro, V.; Furlani, C. *Inorg. Chim. Acta* **1978**, *26*, L11–L12.